Biochemistry and Biophysics Reports 30 (2022) 101250

Contents lists available at ScienceDirect

Biochemistry and Biophysics Reports

journal homepage: www.elsevier.com/locate/bbrep

Wolframin deficiency is accompanied with metabolic inflexibility in rat striated muscles

Kersti Tepp [a,*,1], Jekaterina Aid-Vanakova [a,b,1], Marju Puurand [a], Natalja Timohhina [a], Leenu Reinsalu [a,b], Karin Tein [a,c], Mario Plaas [c], Igor Shevchuk [a], Anton Terasmaa [a], Tuuli Kaambre [a]

[a] Laboratory of Chemical Biology, National Institute of Chemical Physics and Biophysics, Akadeemia tee 23, 12618, Tallinn, Estonia
[b] Department of Chemistry and Biotechnology, School of Science, Tallinn University of Technology, Ehitajate tee 5, 12618, Tallinn, Estonia
[c] Institute of Biomedicine and Translational Medicine, Laboratory Animal Centre, University of Tartu, 14B Ravila Street, Tartu, 50411, Estonia

ARTICLE INFO

Keywords:
Mitochondria
Wolframin
Wolfram syndrome
Skeletal muscle
Heart
Metabolic inflexibility
Energy metabolism

ABSTRACT

The protein wolframin is localized in the membrane of the endoplasmic reticulum (ER), influencing Ca2+ metabolism and ER interaction with mitochondria, but the exact role of the protein remains unclear. Mutations in Wfs1 gene cause autosomal recessive disorder Wolfram syndrome (WS). The first symptom of the WS is diabetes mellitus, so accurate diagnosis of the disease as WS is often delayed. In this study we aimed to characterize the role of the Wfs1 deficiency on bioenergetics of muscles. Alterations in the bioenergetic profiles of Wfs1-exon-5-knock-out (Wfs1KO) male rats in comparison with their wild-type male littermates were investigated using high-resolution respirometry, and enzyme activity measurements. The changes were followed in oxidative (cardiac and soleus) and glycolytic (rectus femoris and gastrocnemius) muscles. There were substrate-dependent alterations in the oxygen consumption rate in Wfs1KO rat muscles. In soleus muscle, decrease in respiration rate was significant in all the followed pathways. The relatively small alterations in muscle during development of WS, such as increased mitochondrial content and/or increase in the OxPhos-related enzymatic activity could be an adaptive response to changes in the metabolic environment. The significant decrease in the OxPhos capacity is substrate dependent indicating metabolic inflexibility when multiple substrates are available.

1. Introduction

The protein wolframin consists of 890 amino acids, and is located in the membrane of endoplasmic reticulum (ER) with nine *trans*-membrane domains [1–3]. Wolframin regulates Ca^{2+} homeostasis, has influence on the formation of mitochondria-associated ER membrane (MAM) and affects Ca^{2+} transport between mitochondria and ER [4–6]. Alterations in intracellular wolframin content are associated with ER stress and activation of the Unfolded Protein Response (UPR) [7–16]. However, the exact mechanism of wolframin function is still not clear [8,17–20].

Mutations in the wolframin coding WFS1 gene cause autosomal recessive disorder Wolfram syndrome 1 (WS1) [21–23]. Usually WS starts with *diabetes mellitus* (DM, mostly during the first decade of the life), followed by optic atrophy (OA, in the beginning of the second decade), *diabetes insipidus (DI)* and deafness (D); therefore acronym DIDMOAD is used. Defects in the CDGSH Iron Sulfur Domain 2 (CISD2, or ERIS (endoplasmic reticulum intermembrane small protein or WFS2) gene, cause progression of illness with symptoms alike WS1, named Wolframin Syndrome type 2 (WS2, approximately 5–10% of the WS cases) [24,25]. However, till now a direct functional interaction between CISD2 and wolframin has not been detected [26,27].

WS first symptom, glucose intolerance, is due to the progressive loss of pancreatic β-cells. This, and simultaneous neuronal tissue degeneration is initiated by ER stress, UPR activation and altered Ca^{2+} homeostasis [28,29]. WS is a rare disease and is doubtlessly underdiagnosed, as after DM symptoms appear, diabetes and its complications are primarily targeted [30].

ER works in close functional interaction with mitochondria. Several symptoms of WS have common features with mitochondrial diseases like Friedreich ataxia and Leber's hereditary optic neuropathy (LHON)

* Corresponding author.
E-mail address: kersti.tepp@kbfi.ee (K. Tepp).
[1] These authors contributed equally to this work.

https://doi.org/10.1016/j.bbrep.2022.101250
Received 10 December 2021; Received in revised form 28 February 2022; Accepted 8 March 2022

[31–33]. Direct mitochondrial DNA (mtDNA) deletions have been observed only in some of WS patients, but the altered regions vary and do not occur in most WS cases [33–36].

Besides nerve and β-cells, the content of the wolframin is high in the heart and skeletal muscles [2]. The role of the wolframin as Ca^{2+} metabolism regulator, and the fact that these muscles relay mostly on mitochondrial energy metabolism should cause strong alterations in the heart and oxidative muscle cells of WS patients. Also, development of the insulin resistance and diabetes in WS patients should be accompanied by changes in both skeletal and heart muscles mitochondria as is described in patients with similar symptoms without WS [31,37]. It is necessary to clarify what modifications have taken place in the bioenergetic profile of skeletal and heart muscle cells in wolframin deficiency. Severe skeletal muscle dysfunction, and shift in muscle type have been detected in WS2 [24,25,38]. In the case of WS1 the reported alterations in the skeletal muscles are milder, if at all, and appear in a later stage of the disease. Structural defects in heart muscle of the WS1 patients is noticed in somewhat higher percentage than in average population but it is not prevailing in all patients [30,39–41]. However, it has been shown that WFS1-deficient rat left ventricle cardiomyocytes had increased contractility (both amplitude and duration of the contraction) due to the prolonged cytosolic calcium transients [18]. Also, a higher relative incidence of sinus tachycardia and atrioventricular arrhythmias has been shown in WS patients [42].

In our previous study we investigated alterations in mitochondrial metabolism of Wfs1KO mice muscles and found decreased and less coupled NADH-linked ADP-stimulated respiration in comparison with wild type (WT) littermates [43]. These alterations were largely substrate-dependent. In Wfs1KO mice muscles the maximal mitochondrial respiration in the presence of Glutamate (Glut) and Malate (Mal) as respiratory system complex I (CI)-linked substrates was decreased in all studied muscle types, accompanied with significantly increased Leak respiration in glycolytic muscles. With Mal and Pyruvate (Pyr) as substrates the increased Leak was detected only in glycolytic muscles (rectus femoris (RF)) and white gastrocnemius (GW)) and decrease in CI linked oxygen consumption was significant only in GW [43,44]. Decrease in adenylate and creatine kinase enzymatic activities of skeletal muscles of wolframin-deficient glucose-intolerant animals and changes in coupling of these enzymes to oxidative phosphorylation (OxPhos) suggest the reconfiguration of energy transport networks and thus could affect muscle performance at higher workloads [43].

Alterations in substrate preferences, detected in WFS1KO mice muscles, agree with the described incapability to use certain available substrates, metabolic inflexibility in diabetes and other metabolic diseases [45]. In diabetic heart, even in hyperglycemic situation, heart muscle cells mostly use fatty acids (FA) [46,47]. In the contrary, the failing heart is metabolically inflexible with increased glucose metabolism [47]. In the skeletal muscle cells of individuals with type-2 diabetes glucose oxidation is elevated and FA usage reduced [48,49].

The extent and severity of the alterations due to the WS in a specific cell type seems not to be directly related to the wolframin content of the cells. Therefore it is possible that some cells have developed adaptation mechanisms to overcome the wolframin deficiency. Knowledge of these means could give us valuable information for the development of better medication for WS. Also, WS1-specific change in the energy metabolism of muscle cells helps to clarify the role of wolframin in cells in different tissues to enable more precise medication.

Generation and characterization of rat model of Wolfram syndrome (Wfs1-exon-5 KO, Wfs1KO), used in this study was described earlier [50]; exon 5 of Wfs1 gene is deleted in this model and results in appearance of WS symptoms [50]. This is a loss of function model and the order of appearance of WS symptoms is similar to the WS development in humans. First, a decrease in glucose-stimulated insulin release is detected from 3 month of age in this Wfs1KO rat model, glucose intolerance progresses with age and culminates with severe hyperglycemia and insulin dependent diabetes mellitus at the age of 12 months [50]. From this age also brainstem and optic nerve neurodegeneration is observed. Diabetes mellitus and optic nerve atrophy appears in childhood or puberty for most of human WS patients, while in the rat model WS symptoms appear after sexual maturity. Drawing of direct parallels from rat studies to human patients must always be done with caution, such limitation is inherent for any animal model of human disease. However, this is unlikely to affect conclusion of this study on the role of Wfs1 on muscle bioenergetics.

The aim of our research is to determine the alterations in bioenergetics profile of the wolframin deficient muscle and clarify the role of the wolframin in the muscle energy metabolism.

2. Methods

2.1. Laboratory animals and chemicals

In all the experiments we used wild type (WT) male Wistar rats and their Wfs1-deficient male littermates (age 8–9 months). Wfs1-deficient rats were generated by deletion of exon 5 in Wfs1 gene resulting in loss of 27 amino acids from the Wfs1 protein, and loss of function of the protein [50]. Breeding and genotyping of the rats were performed at the Laboratory Animal Centre of the Institute of Biomedicine and Translational Medicine, University of Tartu. The rats were housed under standard laboratory conditions (at constant temperature 22 °C and a 12:12 h light/dark cycle with free access to food and water). Animal experiments were approved by the Estonian National Board of Animal Experiments (protocol nr. 114 from 13.10.2017) in accordance with the European Communities Directive (86/609/EEC).

Only ultra-pure chemicals suitable for molecular biology and work with cell cultures were used in experiments. All chemicals were purchased from Fluka and Sigma-Aldrich (Saint Louis, MO, USA).

2.2. Preparation of skinned muscle fibers

For fiber preparation animals were anaesthetized by intraperitoneal injection of ketamine (75 mg/kg) and dexmedetomidin (1 mg/kg), decapitated. Permeabilized fibers were prepared from the heart, *m. soleus*, GW and RF according to the methods described previously [51]. The cells' sarcolemma was permeabilized by saponin treatment (50 μg/mL) for 30 min at 4 °C. Fibers were washed in Mitomedium B solution: EGTA (0.5 mM), $MgCl_2.6H_2O$ (3.0 mM), K-lactobionate (60 mM), KH_2PO_4 (3.0 mM), taurine (20 mM), HEPES (20 mM), sucrose (110 mM), dithiothreitol (DTT, 0.5 mM), bovine serum albumin (BSA, 5 mg/ml)) at pH 7.1 supplemented with leupeptin (5 μM) for the protection of cytoskeletal proteins from lysosomal proteolysis and kept in the same solution at 4 °C under constant stirring until used for experiments.

2.3. Measurements of oxygen consumption

All measurements of oxygen consumption were performed by a high-resolution respirometry instrument Oxygraph-2K (OROBOROS Instruments, Innsbruck, Austria). Experiments were carried out at 25 °C in the Mitomedium B solution [52], supplemented with BSA (5 mg/mL) under continuous magnetic stirring. The permeabilized fiber was weighted and inserted into the oxygraphic chamber with respiration media (Mitomedium B solution) supplemented with respiratory substrates according to the protocol. The measured oxygen consumption rates are presented as nmolO_2/min per mg wet weight.

2.4. Respiratory complexes protocol (RC)

In order to compare the individual capacity of the ETS complexes in relation to two substrate pathways, the classical protocol for measurement of respiratory complexes was applied. All the concentrations presented in the following protocols are final concentrations in the oxygraphic camber.

Permeabilized muscle fibers were inserted into an oxygraph chamber filled with Mitomedium B solution supplemented with Mal (2 mM). First either Glut (Protocol 1A) or Pyr (Protocol 1B) was added to record basal Leak respiration in the absence of adenylates. Then in both protocols ADP (2 mM) was added and the respiratory capacity of ETS complex I (CI) was measured. After inhibition of CI with rotenone (Rot, 2.5 μM) the activity of complex II (CII) was determined in the presence of CII-dependent substrate, succinate (Suc, 10 mM). Then ETS complex III was inhibited with Antimycin A (AntA, 10 μM) and addition of N,N,N′, N′-tetramethyl-p-phenylenediamine (TMPD; 1 mM) demonstrates maximal capacity of complex IV (CIV). Finally, addition of NaCN (1 mM) inhibited cytochrome oxidase (COX) and blocked electron transport; as a result it allowed detecting residual oxygen consumption due to TMPD oxidation reaction.

2.5. Substrate-uncoupler-inhibitor titration (SUIT) protocols

To clarify the task of separate substrate branches of OxPhos and maximal respiratory capacity in the presence of multiple substrates, following modified SUIT protocols were used [53].

The SUIT-1 protocol was applied to determine the role of FA oxidation linked OxPhos independently from glucose-linked pathway. In this protocol firstly Mal and octanoyl carnitine (Oct, 0.2 mM) were injected into the chamber to register basal Leak oxygen consumption, after that ADP (2 mM) was added to stimulate phosphorylation system. To complement the system with substrate from glycolytic pathway, Pyr (5 mM) was inserted. In order to detect maximal capacity of CI, Glut (5 mM) was added into the chamber. Addition of Suc (10 mM) allowed to measure the ADP-dependent respiration when electrons are fed simultaneously to the ETS via CI and CII. Subsequent addition of ADP (final concentration of 5 mM) allowed controlling the limitations in the efficiency of ATP synthase [54]. The maximal capacity of the ETS was evaluated with titration of uncoupler carbonyl cyanide-4-(trifluoromethoxy) phenylhydrazone (FCCP) until saturation of respiration was reached. Subsequent inhibition of CI by Rot (2.5 μM) allowed to determine the CII-linked electron transfer capacity. Inhibition of Complex III (CIII) by AntA (10 μM) allowed to determine the residual oxygen consumption.

In the third, SUIT-2 protocol, to control whether the contribution of glycolytic substrate pathway could have inhibitory influence on the ETS, the substrates were presented in reverse way. First Mal with Pyr was introduced, then, after registration of Leak respiration, ADP-dependent oxygen consumption was determined. Next, Oct was injected and combined CI-substrate linked respiration was detected. Maximum CI-linked oxygen consumption rate was measured with the Glut. At the end, the CII-linked substrate Suc was added to activate ETS CII-dependent respiration.

In the fourth, SUIT-3 protocol, maximal capacity of glucose-linked substrate pathway was determined independently from FA pathway. First Mal with Pyr was introduced into the chamber, then, after registration of Leak respiration, ADP-dependent oxygen consumption was determined. After that, maximum rate of NADH-linked oxygen consumption was measured with the Glut. Then, in the presence of CII-linked substrate Suc joint CI and CII-dependent respiration was registered. Finally, the capacity of ETS was evaluated by titration with FCCP.

2.6. Energy transfer pathways

To determine the alterations in the energy transfer pathways, the influence of AK or CK pathway activation on the mitochondrial respiration was measured. For that, after injection of substrates Mal and Glut, ATP-ases were activated with MgATP (2 mM in oxidative and 0.1 mM on glycolytic muscles). After that, addition of 10 mM Cr or 2 mM AMP activated the respective pathways and an increase in respiratory rate indicates an association between the respective energy transfer network and OxPhos [52].

2.7. Determination of enzymatic activities

2.7.1. Preparation of cell lysates

Pieces of muscles were snap frozen in liquid nitrogen and stored at −80 °C. Tissues were grinded in liquid nitrogen with pestle and homogenized in the Tris-HCl (pH = 8.1), the medium containing KCl (0.9 M), glucose (10 mM), $MgCl_2$ (20 mM), EDTA-Na_2 (10 mM), Triton X-100 (0.25%) and leupeptin (5 μg/mL), at pH 8 using a Retsch Mixer Mill (Retsch) at 25 Hz for 2 min, then centrifuged at 12,000 rcf for 20 min at 4 °C. The supernatants were used for enzymatic assays. Protein concentrations were determined by Pierce BCA Protein Assay Kit according to the manufacturer recommendations using bovine serum albumin (BSA) as a standard.

2.7.2. Measurements of activities

Determination of HK activity was performed using a spectrophotometer (PerkinElmer, U.S.) in solution containing Tris–HCl (50 mM), KCl (45 mM), NaH_2PO_4 (1 mM), EDTA-Na_2 (0.5 mM), $MgCl_2$ (7.7 mM) glucose (4.2 mM), NADP (0.6 mM), MgATP (6.7 mM), glucose-6-phosphate dehydrogenase (G6PD) (1 IU/mL), adjusted at 25 °C. The rate of NADPH formation was monitored after addition of homogenate at 340 nm [55].

ETS Complex I activity was measured with spectrophotometer (PerkinElmer, U.S.) from homogenates in phosphate buffer (100 mM, pH 7.4) comprising NADH, Coenzyme Q1 stock B, KCN, and NaN_3 ca. 100 s. At the end rotenone was added to record rotenone insensitive activity of the preparation [56].

Citrate synthase activity was measured spectrophotometrically in cell lysates at 25 °C with a FLUOstar Omega microplate reader. Citrate synthase (CS) activity was determined by measuring the rate of thionitrobenzoic acid production at 412 nm [57].

2.8. DNA extraction and mitochondrial DNA (mtDNA) copy number

DNA was isolated from frozen rat muscle tissue samples using PureLinkTM Genomic DNA Mini Kit (Invitrogen, USA) according to the instructions provided by the manufacturer. DNA concentrations and quality were measured using the BioSpec-Nano spectrophotometer (Shimadzu, Japan).

The DNA from muscles was used to determine the mitochondrial DNA copy number by the comparison of mitochondrial and nuclear DNA measured by real-time PCR using the Rat Mitochondrial DNA Copy Number Kit (MCN2) (Detroit R&D, USA). The manufacturer's instructions were followed to prepare samples for PCR and to calculate the mtDNA copy number relative to nucDNA.

3. Results

In this study we determined alterations in the bioenergetic profile of the two oxidative (heart, soleus) and two glycolytic (RF and GW) muscles of the 8–9 month old Wfs1 deficient rats in comparison to WT littermates. To characterize alterations in the ETS profile, we measured sequential activation of ETS complexes and ADP-dependent oxygen consumption rate. We evaluated flexibility of OxPhos with different substrate combinations to switch between glucose-linked (Pyr) and FA (Oct) substrates.

First we determined oxygen consumption capacity for respiratory chain complexes CI, CII and CIV individually (RC protocol, Fig. 1), using respective substrates/inhibitors (two alternative CI-linked substrate combinations: Mal with Glut and Mal with Pyr). We did not register any statistically significant alteration in Wfs1KO muscles in comparison with WT animals for either substrate combination (Table 1 in Supplements).

Next we applied SUIT protocols where multiple ETS complexes are activated simultaneously, a situation which is more in line with *in vivo* conditions. At the beginning of the SUIT-1 protocol respiration is supported only by the FA pathway with Oct. In this state in the heart muscle

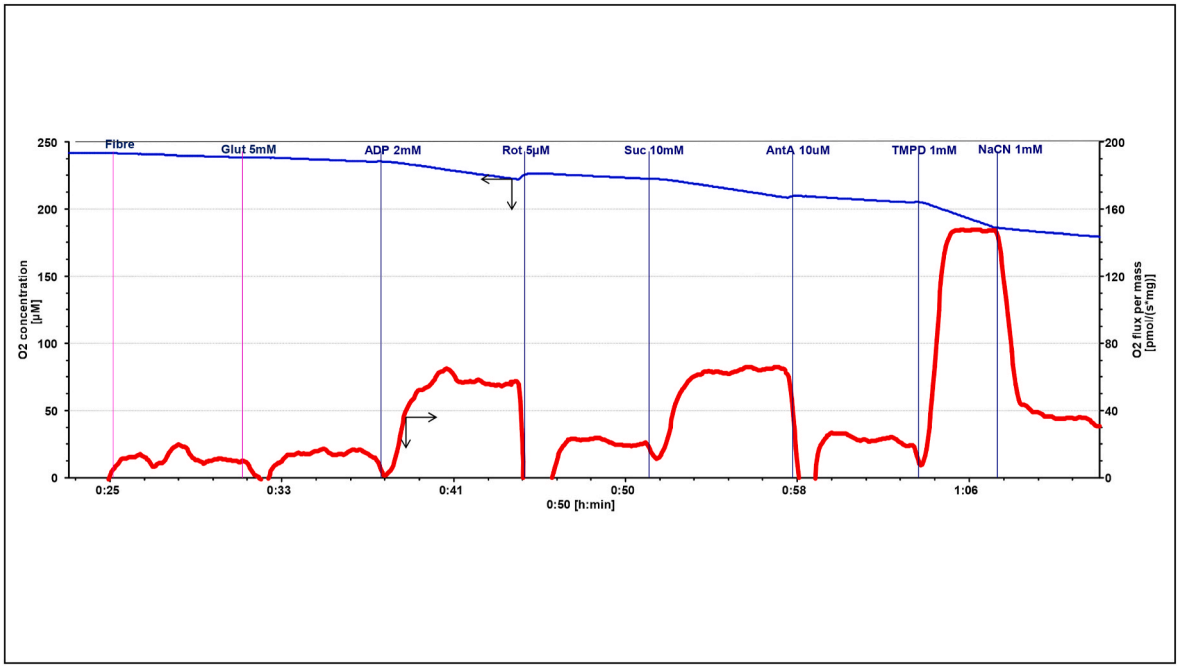

Fig. 1. Representative trace of oxygraphic measurement. Analysis of the individual respiratory chain complexes activities.
After insertion of the muscle fiber into the oxygraphic chamber we added CI – linked substrate glutamate (Glut, 5 mM; malate (2 mM) is in the medium), and the basal oxygen consumption rate without adenylates (Leak) is visible. Then the addition of ADP (2 mM) activates ATP-Synthase (maximal respiration via complex I (CI)). Thereafter, we inhibited CI with its specific inhibitor rotenone (Rot, 5 µM), added succinate (Succ, 10 mM) and registered maximal oxygen consumption capacity through CII. After insertion of antimycin A, (AntA, 10 µM), an inhibitor of complex III, we injected N,N,N',N'-tetramethyl-p-phenylenediamine (TMPD, 1 mM) and ascorbate (5 mM) to activate cytochrome c oxidase associated oxygen consumption, demonstrating the theoretical maximal respiration rate. Thereafter, we added Na cyanide (NaCN) to inhibit cytochrome c oxidase. Blue line – oxygen concentration in the medium, red line – oxygen consumption rate.

Table 1
Enzymatic activities of the wolframin-deficient (Wfs1KO) and wild type (WT) rat heart, m. soleus, m. rectus femoris (RF) and m. gastrocnemius white (GW) fibers.

Enzyme	Muscle	WT		Wfs1KO	
Citrate synthase µmol/mg protein	Heart	156.3	±9.8	156.9	±9.0
	Sol	44.3	±2.5	63.1	±5.7*
	RF	15.4	±0.9	17.1	±0.9
	GW	19.0	±2.3	29.0	±2.8**
Hexokinase µmol/mg protein	Heart	53.7	±2.6	60.3	±2.3
	Sol	28.1	±0.7	32.8	±0.5
	RF	8.2	±0.5	8.9	±0.5
	GW	7.9	±0.5	8.1	±0.5
Complex I µmol/mg protein	Heart	438.0	±26.6	489.2	±51.4
	Sol	190.4	±7.3	220.2	±14.8
	RF	11.9	±0.9	20.6	±1.8**
Complex I/CS	Heart	2.8	±0.2	3.1	±0.4
	Sol	4.3	±0.3	3.5	±0.4
	RF	0.8	±0.1	1.2	±0.1*

**$p < 0.01$; *$p < 0.05$; $n = 6–10$.

there was no difference in FA-linked respiration rate between WT and Wfs1KO. In contrast, in soleus, which also represents oxidative striated muscle, there was a clear decline in the respiratory rate with Oct in Wfs1KO animal (Fig. S1 in Supplements). Following the protocol, CI-linked respiration was then activated. Registered maximal CI-linked respiration and maximal OxPhos (CI + CII) were significantly reduced in both oxidative muscles of Wfs1KO compared to the WT (p=<0.01 (Fig. 2); and p=<0.01 (Fig. S1 in Supplements);), for heart and soleus, respectively). In the normal heart, the sequential addition of substrates was followed by an increase in respiration rate and peaked at the highest level in the presence of the uncoupler (Fig. S1 in Supplements), reflecting the plasticity and the ability of mitochondrial energy metabolism to use different substrates simultaneously. This plasticity appears to be altered in Wfs1KO animals and expresses as loss in efficiency to use glucose-linked carbon sources if mitochondria are already switched to FA oxidation. At the same time, when the same protocol was applied to glycolytic muscles there was no significant differences in the OxPhos rates in a situation when FA oxidation were activated before glucose-linked pathway of Wfs1KO in comparison with WT.

We determined whether the decrease in the respiration rate with the glucose-linked substrate in oxidative muscle was caused by the FA pathway that inhibited utilisation of other CI-linked substrates with SUIT-2 protocol. We activated the pathways in the reversed order where the glucose-linked substrate, Pyr was added first. At these conditions no significant alteration was detected in Wfs1KO heart muscle (Fig. 2, Fig. S1 in Supplements) suggesting that FA pathway activation was the one that inhibited the glucose-linked pathway in the SUIT1 protocol. However, the OxPhos rates of the Wfs1KO soleus muscle are significantly decreased regardless of the order of added substrates (p=<0.01, Fig. 2; Table 1 in Supplements).

In glycolytic muscles, the maximal OxPhos capacity of the RF with SUIT2 protocol was lower in Wfs1KO rat ($p < 0.05$), whereas in the Wfs1KO GW muscle the CI-linked and maximal OxPhos capacity was even increased compared to WT ($p < 0.05$ and $p < 0.01$ respectively; Fig. 2). To the contrary of the WT RF muscle, in GW the addition of Oct after Pyr did not increase the respiration rates of WT and Wfs1KO rat GW to the level at which they reached when the substrates were added in reversed order (Fig. 2).

We used SUIT-3 protocol to determine alterations in the use of the glucoses-linked substrate pathway. In the heart muscle there was no significant differences in the ETS capacity between Wfs1KO and WT when Pyr was used as a substrate. Again, reduced OxPhos rate was registered in soleus muscle of Wfs1KO rat ($p < 0.01$), and no significant change were observed in the ETS capacity in glycolytic muscles of Wfs1KO animals (Fig. 2).

When comparing different substrate introduction orders within one muscle type only, some tendencies can be observed. In WT heart muscle

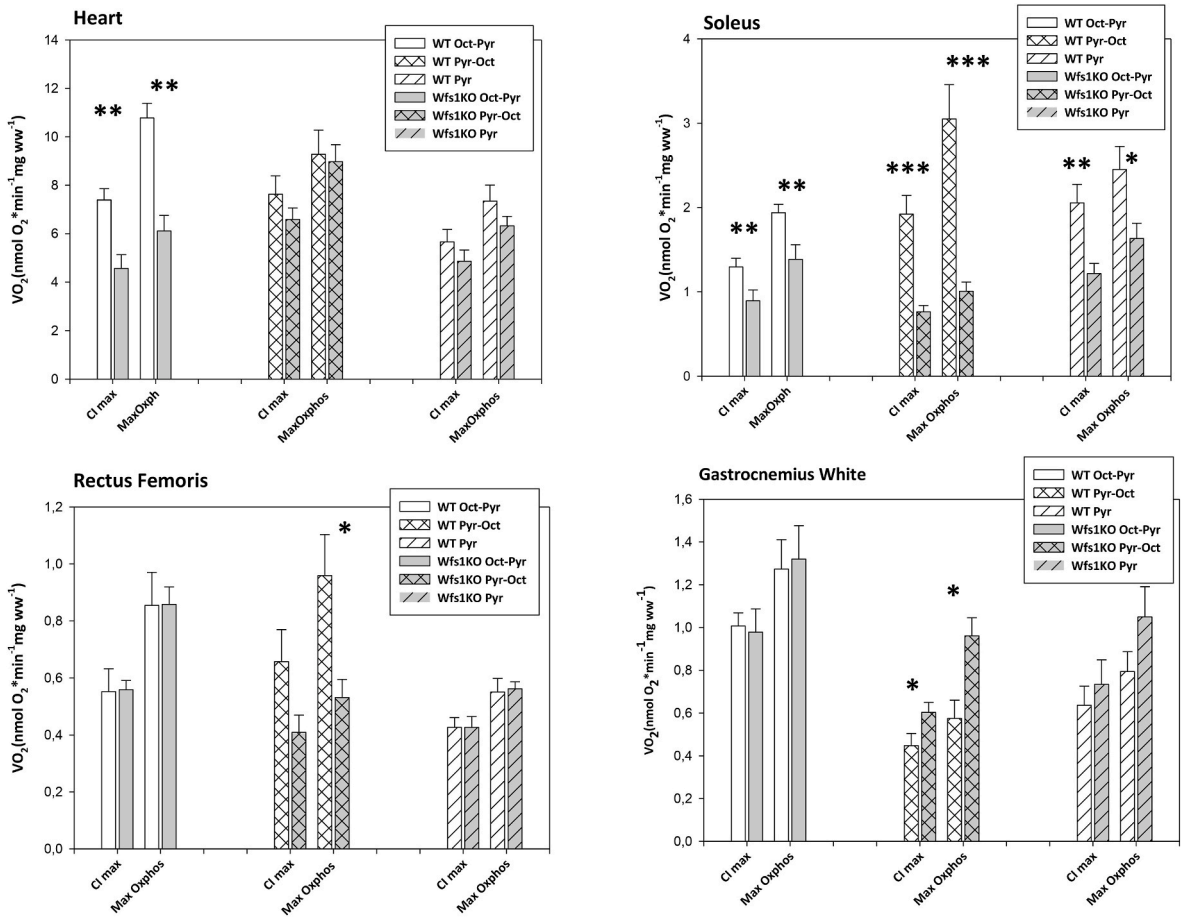

Fig. 2. OxPhos capacity through CI and maximal OxPhos values with simultaneously activated CI and CII - linked substrate pathways. Maximal oxygen consumption rates with CI- linked substrates (CI) and in the presence of simul
-taneously
activated complex I (CI) and CII-linked substrates (Max OxPhos) in wolframin-deficient (Wfs1KO) and wild type (WT) rat heart, m. s
oleus, m. r
ectus femoris (RF) and m. g
astrocnemius white (GW) fibers. In order to investigate the influence of multiple substrate pathways to the respiratory capacity, we used CI-linked substrates in variable order: in SUIT1 protocol (Oct-Pyr), first we inserted fatty acid - octanoyl carnitine (Oct, 0.2 mM), then added glucose-linked pathway substrate pyruvate (Pyr, 5 mM), para id="fspara0065">mM). In SUIT2 protocol (Pyr-Oct) first Pyr was introduced, then we added Oct, followed by Glut. In SUIT3 (Pyr) protocol we first injected Pyr and then Glut. In all the protocols malate (Mal, 2 mM) was in the medium and succinate (10 mM) was used as CII-linked substrate. Respiration rates are represented as nmol O2*min-1*mg ww-1; ***p <
0.001; **p <
0.01; *
p < 0.05; n = 6–
10.

the maximal OxPhos capacity as well as CI-linked respiration rate is higher with SUIT1 and SUIT2 protocol (with Oct; $p < 0.05$) than with SUIT3 (without Oct). In case of Wfs1KO heart muscle the highest oxygen consumption rate was detected with SUIT2 protocol (Pyr added first) in comparison with SUIT1 and SUIT3 ($p < 0.05$), indicating the alterations in fatty acid pathway. In WT glycolytic RF muscle there is a tendency to achieve higher maximal oxygen consumption rate in the presence of Oct and Pyr than with Pyr alone ($p < 0.05$). In contrast, in Wfs1KO RF muscle the OxPhos rates with SUIT2 as well as SUIT3 (just Pyr) protocol are lower in comparison with the situation when the fatty acid pathway is activated first, followed by Pyr (SUIT1 protocol ($p < 0.05$)), indicating an inhibitory effect of glycolysis-linked pathway on FA pathway.

To determine whether the fall in the oxygen consumption rate present with CI-linked substrates in heart, soleus and RF muscle were caused by a possible decrease in CI enzymatic activity the corresponding measurements were performed. No significant difference was found between WT and Wfs1KO muscle (Table 1). Also, in order to check for alterations in the initial metabolic processing of intracellular glucose, we measured HK activity but no difference in Wfs1KO muscle was found (Table 1).

To assess differences in the amount of muscle tissue mitochondria the measurements of citrate synthase (CS) activity were performed. Significantly higher CS activity was detected in the GW and soleus muscle of Wfs1KO in comparison with WT and a similar trend was observed in RF, while there were no changes in heart muscle (Table 1). We also measured mtDNA content relative to nuclear DNA to determine whether the relatively unchanged respiratory capacity in the heart muscle was also consistent with unchanged mitochondrial content. Slightly higher mtDNA content was detected in WFS1KO rat heart muscle in comparison with WT.

Additionally, we performed oxygraphic measurements to identify possible modifications in energy transfer pathways in Wfs1KO muscles. We did not find any substantial alterations in parameters characterizing coupling between AK and CK energy transfer pathways and OxPhos

(Table S2 in Supplements).

4. Discussion

Heart and skeletal muscle cells have high wolframin abundance [2]. However, functional impact of Wfs1 deficiency in muscles is poorly studied. Ataxia and respiratory problems of WS patients are assumed to be directly related with neurodegeneration, not to the alterations in muscle metabolism. Though, there are few reports demonstrating altered cardiac function in WS patients e.g. incidences of cardiac murmurs [30,58]. One case was documented in Tunisia - a patient with moderate WS is accompanied with cardiomyopathy [59]. Disturbed cardiac calcium signalling and cardiac function was also reported in a rat model of WS [18]. Our aim was to determine bioenergetics profile of Wfs1 deficient heart and skeletal muscles.

In this study, 8–9 month old Wfs1KO rats were used. Previous research has shown that glucose intolerance and defective insulin secretion develops at the age of 7 month while basal blood and urine glucose levels are still normal [50]. The age was chosen to avoid artifacts related to elevated blood glucose. In order to investigate the alterations in muscles of different metabolic type we used two oxidative (heart and soleus) and two glycolytic (RF and GW) muscles.

The bioenergetic profile of a tissue is characterized via measurement of mitochondrial oxygen consumption, which depends on two main substrate delivery pathways: FA oxidation and glycolysis-linked pathway. Every cell has its substrate pathway preference, but in healthy tissue most of the cell types are able to shift between the substrates according to the metabolic situation. Inflexibility between these pathways is a hallmark in several metabolic diseases [45,47]. Similarly, decrease in the activity of some of the respiratory system complexes could be partly compensated by another. For example, increased CII activity accompanied with decreased CI one, is described in several tissues during aging and in the case of pathology [60–63].

Our study did not detect significant increase in the Leak oxygen consumption, indicating that functionality of the inner mitochondrial membrane of the muscles is not extensively altered in Wfs1 deficiency. Also, there were no significant alterations in maximal oxygen consumption capacity of individual respiratory complexes in oxidative muscles.

In Wfs1KO heart muscle the main alteration was inhibitory effect of activated FA pathway to the glucose-linked pathway usage. Our results are compatible with the previous knowledge that the energy production in the insulin resistant heart cells cannot effectively switch from FA to glucose-linked metabolism and rely primarily on FA oxidation, even in hyperglycaemic state [37,46,47]. Wfs1KO rats have insulin deficiency, while insulin sensitivity is not altered. Thus, these changes in heart muscle bioenergetics can be caused by insulin deficiency or Wfs1 deficiency, but not by insulin insensitivity. Interestingly, when the substrates are introduced in reversed order and the glucose-linked substrate pathway is activated before FA pathway, there was no difference between Wfs1KO and WT in the heart muscle fibre. The relatively small alteration in the heart muscle oxygen consumption could be explained by slightly increased mtDNA relative to nucDNA ratio in the heart muscle of Wfs1KO animals, indicating elevated mitochondrial content in Wfs1KO rats' heart (Table S2 in Supplements). Similar results have been demonstrated in mice genetic model of type-1 diabetes [64].

In other oxidative muscle *m. soleus*, there was a significant decrease in the respiratory capacity of Wfs1KO animals with all substrate combinations and it was not related to the order in which the substrates were presented. Higher CS activity in Wfs1KO soleus muscle also suggests an adaptive increase in the number of mitochondria in response to a decrease in ETS capacity. However, these changes do not appear to be sufficient to maintain OxPhos level similar to that in WT. The activity of CI in both oxidative muscles does not differ between Wfs1KO and WT rat, so the declined OxPhos capacity in these tissues is not related to the decreased activity of this ETS complex.

In both glycolytic muscles studied, we found slightly higher individual RC complexes respiratory rates in Wfs1KO muscles which is accompanied with increased CS activity of tissue.

In contrast to the heart muscle, Wfs1KO RF muscle display an inhibitory effect of glucose-linked pathway on FA usage. Similar phenomena, elevated glucose oxidation and reduced FA usage, is described also in the skeletal muscle cells of individuals with type-2 diabetes and other metabolic diseases [48,49,65]. The bioenergetics profile of Wfs1KO GW muscle indicates adaptive rearrangements in tissue level, as both CS activity and therefore also oxygen consumption rates per tissue mass have increased. Similar changes in muscle fibre type were described in RF muscle of Wfs1 deficient mice [44].

Altogether, the most common alteration in the bioenergetics of the muscle cells, caused by the wolframin deficiency is metabolic inflexibility in substrate usage (Fig. 3).

In Wfs1KO heart muscle the glucose-linked pathway is impaired when the FA pathway is activated first. But in glycolytic RF muscle, the activation of glucose-linked pathway blocks the FA usage. Interestingly, in oxidative soleus muscle the decrease in the OxPhos capacity is irrespective to the substrate pathway, while in glycolytic GW, higher CS activity preserves the OxPhos capacity in Wfs1KO muscle. Similar shift is visible in glycolytic RF muscle where in Wfs1KO muscle has higher CI activity than in WT.

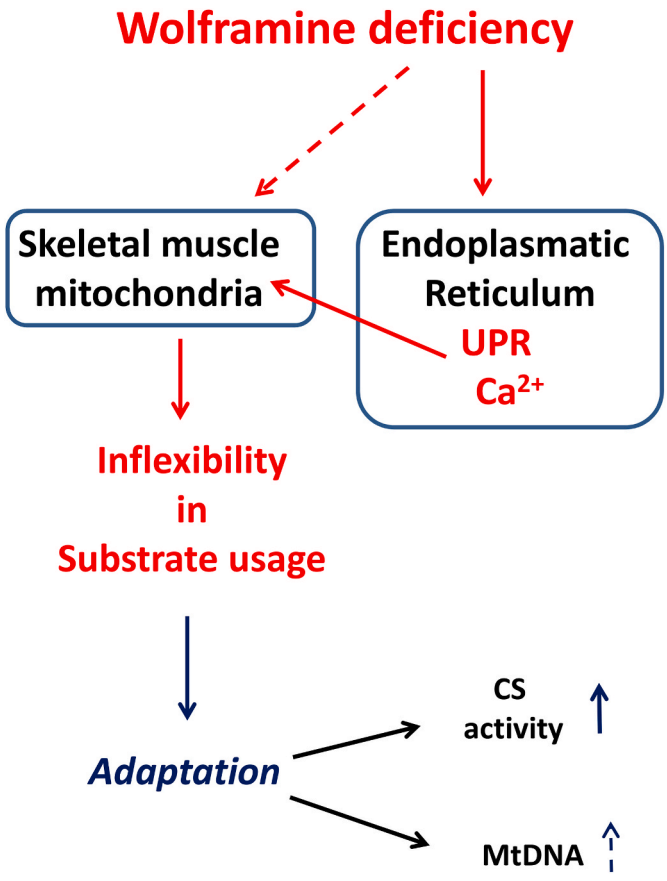

Fig. 3. Alterations in the bioenergetics profile in the rat muscle due to the WFS1 deficiency Wolframin
-deficiency alters Ca2+ metabolism and unfolded protein response (UPR) in endoplasmic reticulum. This initiates abnormalities in the OxPhos substrate use profile, leading to a loss of metabolic flexibility. The relatively small alterations like an increased mitochondrial content and/or increase in the
activities of some OxPhos-related enzymes
in skeletal and heart muscle during development of WS could be may be adaptive changes initiated by alterations in the metabolic environment:.
MtDNA – mitochondrial DNA; CS - citrate synthase.

This study demonstrates that the lack of wolframin doesn't cause universal changes in different muscles. However, deficiency of this protein contributes to the development of metabolic inflexibility in striated muscle tissue. In addition, the ability of mitochondria to use different substrate simultaneously is impaired. It remains to be investigated whether such metabolic inflexibility contributes to WS associated neuronal loss.

Author contributions

Conceptualization, Kersti Tepp, Jekaterina Aid-Vanakova and Anton Terasmaa; Formal analysis, Kersti Tepp; Investigation, Kersti Tepp, Jekaterina Aid-Vanakova, Marju Puurand, Natalja Timohhina, Leenu Reinsalu and Karin Tein; Methodology, Kersti Tepp and Jekaterina Aid-Vanakova; Resources, Mario Plaas; Supervision, Tuuli Kaambre; Visualization, Igor Shevchuk; Writing – original draft, Kersti Tepp and Jekaterina Aid-Vanakova; Writing – re-view & editing, Marju Puurand, Karin Tein, Mario Plaas, Anton Terasmaa and Tuuli Kaambre. All authors have read and agreed to the manuscript.

Declaration of competing interest

The authors declare that they have no known competing financial interests or personal relationships that could have appeared to influence the work reported in this paper.

Acknowledgments

This research was funded by grant PSG471 (Mario Plaas) from Estonian Research Council.

Appendix A. Supplementary data

Supplementary data to this article can be found online at https://doi.org/10.1016/j.bbrep.2022.101250.

References

[1] K. Takeda, H. Inoue, Y. Tanizawa, Y. Matsuzaki, J. Oba, Y. Watanabe, K. Shinoda, Y. Oka, WFS1 (Wolfram syndrome 1) gene product: predominant subcellular localization to endoplasmic reticulum in cultured cells and neuronal expression in rat brain, Hum. Mol. Genet. 10 (2001) 477–484, https://doi.org/10.1093/hmg/10.5.477.

[2] S. Hofmann, C. Philbrook, K.D. Gerbitz, M.F. Bauer, Wolfram syndrome: structural and functional analyses of mutant and wild-type wolframin, the WFS1 gene product, Hum. Mol. Genet. 12 (2003) 2003–2012, https://doi.org/10.1093/hmg/ddg214.

[3] L. Li, L. Venkataraman, S. Chen, H. Fu, Function of WFS1 and WFS2 in the central nervous system: implications for Wolfram syndrome and alzheimer's disease, Neurosci. Biobehav. Rev. 118 (2020) 775–783, https://doi.org/10.1016/j.neubiorev.2020.09.011.

[4] M. Cagalinec, M. Liiv, Z. Hodurova, M.A. Hickey, A. Vaarmann, M. Mandel, A. Zeb, V. Choubey, M. Kuum, D. Safiulina, E. Vasar, V. Veksler, A. Kaasik, Role of mitochondrial dynamics in neuronal development: mechanism for Wolfram syndrome, PLoS Biol. 14 (2016), e1002511, https://doi.org/10.1371/journal.pbio.1002511.

[5] B. Delprat, T. Maurice, C. Delettre, Wolfram syndrome: MAMs' connection? Cell Death Dis. 9 (2018) 364, https://doi.org/10.1038/s41419-018-0406-3.

[6] C. La Morgia, A. Maresca, G. Amore, L.L. Gramegna, M. Carbonelli, E. Scimonelli, A. Danese, S. Patergnani, L. Caporali, F. Tagliavini, V. Del Dotto, M. Capristo, F. Sadun, P. Barboni, G. Savini, S. Evangelisti, C. Bianchini, M.L. Valentino, R. Liguori, C. Tonon, C. Giorgi, P. Pinton, R. Lodi, V. Carelli, Calcium mishandling in absence of primary mitochondrial dysfunction drives cellular pathology in Wolfram Syndrome, Sci. Rep. 10 (2020) 4785, https://doi.org/10.1038/s41598-020-61735-3.

[7] H. Ishihara, S. Takeda, A. Tamura, R. Takahashi, S. Yamaguchi, D. Takei, T. Yamada, H. Inoue, H. Soga, H. Katagiri, Y. Tanizawa, Y. Oka, Disruption of the WFS1 gene in mice causes progressive beta-cell loss and impaired stimulus-secretion coupling in insulin secretion, Hum. Mol. Genet. 13 (2004) 1159–1170, https://doi.org/10.1093/hmg/ddh125.

[8] T. Yamada, H. Ishihara, A. Tamura, R. Takahashi, S. Yamaguchi, D. Takei, A. Tokita, C. Satake, F. Tashiro, H. Katagiri, H. Aburatani, J. Miyazaki, Y. Oka, WFS1-deficiency increases endoplasmic reticulum stress, impairs cell cycle progression and triggers the apoptotic pathway specifically in pancreatic beta-cells, Hum. Mol. Genet. 15 (2006) 1600–1609, https://doi.org/10.1093/hmg/ddl081.

[9] Y. Ohta, A. Taguchi, T. Matsumura, H. Nakabayashi, M. Akiyama, K. Yamamoto, R. Fujimoto, R. Suetomi, A. Yanai, K. Shinoda, Y. Tanizawa, Clock gene dysregulation induced by chronic ER stress disrupts beta-cell function, EBioMedicine 18 (2017) 146–156, https://doi.org/10.1016/j.ebiom.2017.03.040.

[10] S. Morikawa, T. Tajima, A. Nakamura, K. Ishizu, T. Ariga, A novel heterozygous mutation of the WFS1 gene leading to constitutive endoplasmic reticulum stress is the cause of Wolfram syndrome, Pediatr. Diabetes 18 (2017) 934–941, https://doi.org/10.1111/pedi.12513.

[11] J.R. Porter, T.G. Barrett, Monogenic syndromes of abnormal glucose homeostasis: clinical review and relevance to the understanding of the pathology of insulin resistance and beta cell failure, J. Med. Genet. 42 (2005) 893–902, https://doi.org/10.1136/jmg.2005.030791.

[12] S.G. Fonseca, M. Fukuma, K.L. Lipson, L.X. Nguyen, J.R. Allen, Y. Oka, F. Urano, WFS1 is a novel component of the unfolded protein response and maintains homeostasis of the endoplasmic reticulum in pancreatic beta-cells, J. Biol. Chem. 280 (2005) 39609–39615, https://doi.org/10.1074/jbc.M507426200.

[13] D. Takei, H. Ishihara, S. Yamaguchi, T. Yamada, A. Tamura, H. Katagiri, Y. Maruyama, Y. Oka, WFS1 protein modulates the free Ca(2+) concentration in the endoplasmic reticulum, FEBS Lett. 580 (2006) 5635–5640, https://doi.org/10.1016/j.febslet.2006.09.007.

[14] S. Lu, K. Kanekura, T. Hara, J. Mahadevan, L.D. Spears, C.M. Oslowski, R. Martinez, M. Yamazaki-Inoue, M. Toyoda, A. Neilson, P. Blanner, C.M. Brown, C.F. Semenkovich, B.A. Marshall, T. Hershey, A. Umezawa, P.A. Greer, F. Urano, A calcium-dependent protease as a potential therapeutic target for Wolfram syndrome, Proc. Natl. Acad. Sci. U. S. A. 111 (2014) E5292–E5301, https://doi.org/10.1073/pnas.1421055111.

[15] M. Zatyka, C. Ricketts, G. da Silva Xavier, J. Minton, S. Fenton, S. Hofmann-Thiel, G.A. Rutter, T.G. Barrett, Sodium-potassium ATPase 1 subunit is a molecular partner of Wolframin, an endoplasmic reticulum protein involved in ER stress, Hum. Mol. Genet. 17 (2008) 190–200, https://doi.org/10.1093/hmg/ddm296.

[16] A.A. Osman, M. Saito, C. Makepeace, M.A. Permutt, P. Schlesinger, M. Mueckler, Wolframin expression induces novel ion channel activity in endoplasmic reticulum membranes and increases intracellular calcium, J. Biol. Chem. 278 (2003) 52755–52762, https://doi.org/10.1074/jbc.M310331200.

[17] C. Angebault, J. Fauconnier, S. Patergnani, J. Rieusset, A. Danese, C.A. Affortit, J. Jagodzinska, C. Megy, M. Quiles, C. Cazevieille, J. Korchagina, D. Bonnet-Wersinger, D. Milea, C. Hamel, P. Pinton, M. Thiry, A. Lacampagne, B. Delprat, C. Delettre, ER-mitochondria cross-talk is regulated by the Ca(2+) sensor NCS1 and is impaired in Wolfram syndrome, Sci. Signal. 11 (2018), https://doi.org/10.1126/scisignal.aaq1380.

[18] M. Cagalinec, A. Zahradnikova, A. Zahradnikova Jr., D. Kovacova, L. Paulis, S. Kurekova, M. Hot'ka, J. Pavelkova, M. Plaas, M. Novotova, I. Zahradnik, Calcium signaling and contractility in cardiac myocyte of wolframin deficient rats, Front. Physiol. 10 (2019) 172, https://doi.org/10.3389/fphys.2019.00172.

[19] S. Gharanei, M. Zatyka, D. Astuti, J. Fenton, A. Sik, Z. Nagy, T.G. Barrett, Vacuolar-type H+-ATPase V1A subunit is a molecular partner of Wolfram syndrome 1 (WFS1) protein, which regulates its expression and stability, Hum. Mol. Genet. 22 (2013) 203–217, https://doi.org/10.1093/hmg/dds400.

[20] S. Koks, R.W. Overall, M. Ivask, U. Soomets, M. Guha, E. Vasar, C. Fernandes, L. C. Schalkwyk, Silencing of the WFS1 gene in HEK cells induces pathways related to neurodegeneration and mitochondrial damage, Physiol. Genom. 45 (2013) 182–190, https://doi.org/10.1152/physiolgenomics.00122.2012.

[21] T.G. Barrett, S.E. Bundey, A.R. Fielder, P.A. Good, Optic atrophy in Wolfram (DIDMOAD) syndrome, Eye 11 (Pt 6) (1997) 882–888.

[22] T.G. Barrett, S.E. Bundey, Wolfram (DIDMOAD) syndrome, J. Med. Genet. 34 (1997) 838–841.

[23] L. Rigoli, F. Lombardo, C. Di Bella, Wolfram syndrome and WFS1 gene, Clin. Genet. 79 (2011) 103–117, https://doi.org/10.1111/j.1399-0004.2010.01522.x.

[24] Z.Q. Shen, Y.L. Huang, Y.C. Teng, T.W. Wang, C.H. Kao, C.H. Yeh, T.F. Tsai, CISD2 maintains cellular homeostasis, Biochimica et biophysica acta, Mol. Cell Res. 1868 (2021) 118954, https://doi.org/10.1016/j.bbamcr.2021.118954.

[25] N.C. Chang, M. Nguyen, J. Bourdon, P.A. Risse, J. Martin, G. Danialou, R. Rizzuto, B.J. Petrof, G.C. Shore, Bcl-2-associated autophagy regulator Naf-1 required for maintenance of skeletal muscle, Hum. Mol. Genet. 21 (2012) 2277–2287, https://doi.org/10.1093/hmg/dds048.

[26] L. Rigoli, C. Di Bella, Wolfram syndrome 1 and Wolfram syndrome 2, Curr. Opin. Pediatr. 24 (2012) 512–517, https://doi.org/10.1097/MOP.0b013e328354ccdf.

[27] S. Amr, C. Heisey, M. Zhang, X.J. Xia, K.H. Shows, K. Ajlouni, A. Pandya, L.S. Satin, H. El-Shanti, R. Shiang, A homozygous mutation in a novel zinc-finger protein, ERIS, is responsible for Wolfram syndrome 2, Am. J. Hum. Genet. 81 (2007) 673–683, https://doi.org/10.1086/520961.

[28] T.T. Fischer, B.E. Ehrlich, Wolfram syndrome: a monogenic model to study diabetes mellitus and neurodegeneration, Curr. Opin. Physiol. 17 (2020) 115–123, https://doi.org/10.1016/j.cophys.2020.07.009.

[29] M.T. Pallotta, G. Tascini, R. Crispoldi, C. Orabona, G. Mondanelli, U. Grohmann, S. Esposito, Wolfram syndrome, a rare neurodegenerative disease: from pathogenesis to future treatment perspectives, J. Transl. Med. 17 (2019) 238, https://doi.org/10.1186/s12967-019-1993-1.

[30] R. Medlej, J. Wasson, P. Baz, S. Azar, I. Salti, J. Loiselet, A. Permutt, G. Halaby, Diabetes mellitus and optic atrophy: a study of Wolfram syndrome in the Lebanese population, J. Clin. Endocrinol. Metab. 89 (2004) 1656–1661, https://doi.org/10.1210/jc.2002-030015.

[31] M. Cnop, H. Mulder, M. Igoillo-Esteve, Diabetes in Friedreich ataxia, J. Neurochem. 126 (Suppl 1) (2013) 94–102, https://doi.org/10.1111/jnc.12216.

[32] F.V. Pallardo, G. Pagano, L.R. Rodriguez, P. Gonzalez-Cabo, A. Lyakhovich, M. Trifuoggi, Friedreich Ataxia: current state-of-the-art, and future prospects for mitochondrial-focused therapies, Transl. Res. : J. Lab. Clin. Med. 229 (2021) 135–141, https://doi.org/10.1016/j.trsl.2020.08.009.

[33] D. Pilz, O.W. Quarrell, E.W. Jones, Mitochondrial mutation commonly associated with Leber's hereditary optic neuropathy observed in a patient with Wolfram syndrome (DIDMOAD), J. Med. Genet. 31 (1994) 328–330, https://doi.org/10.1136/jmg.31.4.328.

[34] S. Hofmann, R. Bezold, M. Jaksch, B. Obermaier-Kusser, S. Mertens, P. Kaufhold, W. Rabl, W. Hecker, K.D. Gerbitz, Wolfram (DIDMOAD) syndrome and Leber hereditary optic neuropathy (LHON) are associated with distinct mitochondrial DNA haplotypes, Genomics 39 (1997) 8–18, https://doi.org/10.1006/geno.1996.4474.

[35] A. Barrientos, J. Casademont, A. Saiz, F. Cardellach, V. Volpini, A. Solans, E. Tolosa, A. Urbano-Marquez, X. Estivill, V. Nunes, Autosomal recessive Wolfram syndrome associated with an 8.5-kb mtDNA single deletion, Am. J. Hum. Genet. 58 (1996) 963–970.

[36] A. Rotig, V. Cormier, P. Chatelain, R. Francois, J.M. Saudubray, P. Rustin, A. Munnich, Deletion of mitochondrial DNA in a case of early-onset diabetes mellitus, optic atrophy, and deafness (Wolfram syndrome, MIM 222300), J. Clin. Invest. 91 (1993) 1095–1098, https://doi.org/10.1172/JCI116267.

[37] M. Makrecka-Kuka, E. Liepinsh, A.J. Murray, H. Lemieux, M. Dambrova, K. Tepp, M. Puurand, T. Kaambre, W.H. Han, P. de Goede, K.A. O'Brien, B. Turan, E. Tuncay, Y. Olgar, A.P. Rolo, C.M. Palmeira, N.T. Boardman, R.C.I. Wust, T. S. Larsen, Altered mitochondrial metabolism in the insulin-resistant heart, Acta Physiol. 228 (2020), e13430, https://doi.org/10.1111/apha.13430.

[38] Y.F. Chen, C.H. Kao, Y.T. Chen, C.H. Wang, C.Y. Wu, C.Y. Tsai, F.C. Liu, C.W. Yang, Y.H. Wei, M.T. Hsu, S.F. Tsai, T.F. Tsai, Cisd2 deficiency drives premature aging and causes mitochondria-mediated defects in mice, Gene Dev. 23 (2009) 1183–1194, https://doi.org/10.1101/gad.1779509.

[39] M.A. Ganie, B.A. Laway, S. Nisar, M.M. Wani, M.L. Khurana, F. Ahmad, S. Ahmed, P. Gupta, I. Ali, I. Shabir, A. Shadan, A. Ahmed, S. Tufail, Presentation and clinical course of Wolfram (DIDMOAD) syndrome from North India, Diabetic medicine, J. Br. Diabet. Assoc. 28 (2011) 1337–1342, https://doi.org/10.1111/j.1464-5491.2011.03377.x.

[40] H.A. Korkmaz, K. Demir, F. Hazan, M. Yildiz, O.N. Elmas, B. Ozkan, Association of Wolfram syndrome with Fallot tetralogy in a girl, Arch. Argent. Pediatr. 114 (2016) e163–166, https://doi.org/10.5546/aap.2016.eng.e163.

[41] L. Tranebjaerg, T. Barrett, N.D. Rendtorff, in: M.P. Adam, H.H. Ardinger, R. A. Pagon, S.E. Wallace, L.J.H. Bean, G. Mirzaa, A. Amemiya (Eds.), WFS1 Wolfram Syndrome Spectrum Disorder, GeneReviews((R)), Seattle (WA), 1993.

[42] B.T. Kinsley, M. Swift, R.H. Dumont, R.G. Swift, Morbidity and mortality in the Wolfram syndrome, Diabetes Care 18 (1995) 1566–1570, https://doi.org/10.2337/diacare.18.12.1566.

[43] K. Tepp, M. Puurand, N. Timohhina, J. Aid-Vanakova, I. Reile, I. Shevchuk, V. Chekulayev, M. Eimre, N. Peet, L. Kadaja, K. Paju, T. Kaambre, Adaptation of striated muscles to Wolframin deficiency in mice: alterations in cellular bioenergetics, Biochim. Biophys. Acta Gen. Subj. 1864 (2020) 129523, https://doi.org/10.1016/j.bbagen.2020.129523.

[44] M. Eimre, K. Paju, N. Peet, L. Kadaja, M. Tarrend, S. Kasvandik, J. Seppet, M. Ivask, E. Orlova, S. Koks, Increased mitochondrial protein levels and bioenergetics in the musculus rectus femoris of wfs1-deficient mice, Oxid. Med. Cell. Longev. 2018 (2018) 3175313, https://doi.org/10.1155/2018/3175313.

[45] J. Gambardella, A. Lombardi, G. Santulli, Metabolic flexibility of mitochondria plays a key role in balancing glucose and fatty acid metabolism in the diabetic heart, Diabetes 69 (2020) 2054–2057, https://doi.org/10.2337/dbi20-0024.

[46] M. Isfort, S.C. Stevens, S. Schaffer, C.J. Jong, L.E. Wold, Metabolic dysfunction in diabetic cardiomyopathy, Heart Fail. Rev. 19 (2014) 35–48, https://doi.org/10.1007/s10741-013-9377-8.

[47] R.L. Smith, M.R. Soeters, R.C.I. Wust, R.H. Houtkooper, Metabolic flexibility as an adaptation to energy Resources and requirements in health and disease, Endocr. Rev. 39 (2018) 489–517, https://doi.org/10.1210/er.2017-00211.

[48] B.H. Goodpaster, L.M. Sparks, Metabolic flexibility in health and disease, Cell Metabol. 25 (2017) 1027–1036, https://doi.org/10.1016/j.cmet.2017.04.015.

[49] D.E. Kelley, M. Mokan, J.A. Simoneau, L.J. Mandarino, Interaction between glucose and free fatty acid metabolism in human skeletal muscle, J. Clin. Invest. 92 (1993) 91–98, https://doi.org/10.1172/JCI116603.

[50] M. Plaas, K. Seppa, R. Reimets, T. Jagomae, M. Toots, T. Koppel, T. Vallisoo, M. Nigul, I. Heinla, R. Meier, A. Kaasik, A. Piirsoo, M.A. Hickey, A. Terasmaa, E. Vasar, Wfs1- deficient rats develop primary symptoms of Wolfram syndrome: insulin-dependent diabetes, optic nerve atrophy and medullary degeneration, Sci. Rep. 7 (2017) 10220, https://doi.org/10.1038/s41598-017-09392-x.

[51] A.V. Kuznetsov, V. Veksler, F.N. Gellerich, V. Saks, R. Margreiter, W.S. Kunz, Analysis of mitochondrial function in situ in permeabilized muscle fibers, tissues and cells, Nat. Protoc. 3 (2008) 965–976, https://doi.org/10.1038/nprot.2008.61.

[52] M. Puurand, K. Tepp, A. Klepinin, L. Klepinina, I. Shevchuk, T. Kaambre, Intracellular energy-transfer networks and high-resolution respirometry: a convenient approach for studying their function, Int. J. Mol. Sci. 19 (2018), https://doi.org/10.3390/ijms19102933.

[53] D. Pesta, E. Gnaiger, High-resolution respirometry: OXPHOS protocols for human cells and permeabilized fibers from small biopsies of human muscle, Methods Mol. Biol. 810 (2012) 25–58, https://doi.org/10.1007/978-1-61779-382-0_3.

[54] V.A. Saks, V.I. Veksler, A.V. Kuznetsov, L. Kay, P. Sikk, T. Tiivel, L. Tranqui, J. Olivares, K. Winkler, F. Wiedemann, W.S. Kunz, Permeabilized cell and skinned fiber techniques in studies of mitochondrial function in vivo, Mol. Cell. Biochem. 184 (1998) 81–100.

[55] R. Paasuke, M. Eimre, A. Piirsoo, N. Peet, L. Laada, L. Kadaja, M. Roosimaa, M. Paasuke, A. Martson, E. Seppet, K. Paju, Proliferation of Human Primary Myoblasts Is Associated with Altered Energy Metabolism in Dependence on Ageing in Vivo and in Vitro, Oxidative Medicine and Cellular Longevity, vol. 2016, 2016, p. 8296150, https://doi.org/10.1155/2016/8296150.

[56] M. Spinazzi, A. Casarin, V. Pertegato, M. Ermani, L. Salviati, C. Angelini, Optimization of respiratory chain enzymatic assays in muscle for the diagnosis of mitochondrial disorders, Mitochondrion 11 (2011) 893–904, https://doi.org/10.1016/j.mito.2011.07.006.

[57] A. Cormio, F. Guerra, G. Cormio, V. Pesce, F. Fracasso, V. Loizzi, P. Cantatore, L. Selvaggi, M.N. Gadaleta, The PGC-1alpha-dependent pathway of mitochondrial biogenesis is upregulated in type I endometrial cancer, Biochem. Biophys. Res. Commun. 390 (2009) 1182–1185, https://doi.org/10.1016/j.bbrc.2009.10.114.

[58] A. Kadayifci, Y. Kepekci, Y. Coskun, Y. Huang, Wolfram syndrome in a family with variable expression, Acta Med. 44 (2001) 115–118.

[59] N. Mezghani, M. Mnif, E. Mkaouar-Rebai, N. Kallel, I.H. Salem, N. Charfi, M. Abid, F. Fakhfakh, The mitochondrial ND1 m.3337G>A mutation associated to multiple mitochondrial DNA deletions in a patient with Wolfram syndrome and cardiomyopathy, Biochem. Biophys. Res. Commun. 411 (2011) 247–252, https://doi.org/10.1016/j.bbrc.2011.06.106.

[60] K. Tepp, M. Puurand, N. Timohhina, J. Adamson, A. Klepinin, L. Truu, I. Shevchuk, V. Chekulayev, T. Kaambre, Changes in the mitochondrial function and in the efficiency of energy transfer pathways during cardiomyocyte aging, Mol. Cell. Biochem. 432 (2017) 141–158, https://doi.org/10.1007/s11010-017-3005-1.

[61] A. Koit, I. Shevchuk, L. Ounpuu, A. Klepinin, V. Chekulayev, N. Timohhina, K. Tepp, M. Puurand, L. Truu, K. Heck, V. Valvere, R. Guzun, T. Kaambre, Mitochondrial respiration in human colorectal and breast cancer clinical material is regulated differently, Oxid. Med. Cell. Longev. (2017) 1372640, https://doi.org/10.1155/2017/1372640, 2017.

[62] A. Weber, H. Klocker, H. Oberacher, E. Gnaiger, H. Neuwirt, N. Sampson, I.E. Eder, Succinate accumulation is associated with a shift of mitochondrial respiratory control and HIF-1alpha upregulation in PTEN negative prostate cancer cells, Int. J. Mol. Sci. 19 (2018), https://doi.org/10.3390/ijms19072129.

[63] M. Gruno, N. Peet, A. Tein, R. Salupere, M. Sirotkina, J. Valle, A. Peetsalu, E. K. Seppet, Atrophic gastritis: deficient complex I of the respiratory chain in the mitochondria of corpus mucosal cells, J. Gastroenterol. 43 (2008) 780–788, https://doi.org/10.1007/s00535-008-2231-4.

[64] X. Shen, S. Zheng, V. Thongboonkerd, M. Xu, W.M. Pierce Jr., J.B. Klein, P. N. Epstein, Cardiac mitochondrial damage and biogenesis in a chronic model of type 1 diabetes, Am. J. Physiol. Endocrinol. Metab. 287 (2004) E896–E905, https://doi.org/10.1152/ajpendo.00047.2004.

[65] C.E. van den Brom, M.C. Huisman, R. Vlasblom, N.M. Boontje, S. Duijst, M. Lubberink, C.F. Molthoff, A.A. Lammertsma, J. van der Velden, C. Boer, D. M. Ouwens, M. Diamant, Altered myocardial substrate metabolism is associated with myocardial dysfunction in early diabetic cardiomyopathy in rats: studies using positron emission tomography, Cardiovasc. Diabetol. 8 (2009) 39, https://doi.org/10.1186/1475-2840-8-39.